

# Technology Trend of High Efficiency Crystalline Silicon Solar Cells

YOSHIO OHSHITA<sup>1</sup>, TAKEFUMI KAMIOKA<sup>1</sup>, AND KYOTARO NAKAMURA<sup>2</sup>

<sup>1</sup>TOYOTA TECHNOLOGICAL INSTITUTE, 2-12-1 HISAKATA, TEMPAKU, NAGOYA 468-8511, JAPAN

<sup>2</sup>MEIJI UNIVERSITY, 1-1-1 HIGASHIMITA, TAMA, KAWASAKI, 214-8571, JAPAN

## ABSTRACT

The conversion efficiencies of crystalline silicon (Si) solar cells are increasing and the module price is dramatically going down. PERC (passivated emitter and rear cell) solar cells, which have achieved high conversion efficiencies of over 20%, are the next main focus for mass production. In the structure of a typical PERC, the minority carrier recombination rate is decreased by the rear side passivation. On the other hand, the hetero-junction of amorphous Si and crystal Si shows high passivation quality at the interface, and an increase in the open circuit voltage. The back-contact cell increases the photo-induced current density because of the shadow loss suppression. The combination of the hetero-junction and the back contact structures realize the 26.33% conversion efficiency. To reduce the fabrication cost of solar cells with high conversion efficiency, passivated contact cells have been proposed. The minority carrier recombination is suppressed by an intermediated layer, such as SiO<sub>2</sub>, between the Si crystal and the contact materials. When the light is irradiated, the current flows through this inter-layer by the tunneling phenomena. High current density and high open circuit voltage are realized by adjusting the work functions of the contact materials.

## INTRODUCTION

Crystalline silicon (Si) solar cells are approaching a major technological turning point. At present, a conventional crystalline Si solar cell is a simple, large size p-n diode with a passivation layer of Si<sub>3</sub>N<sub>4</sub> at the front cell surface. Texturing and an anti-reflective coating (ARC) decreases the reflection of sunlight at the surface. The front side contact metal is silver (Ag) and the back side one is aluminum (Al), which are formed by the screen printing and the firing processes. The maximum conversion efficiency

of this type of solar cell is around 19%; it is difficult to achieve a higher efficiency exceeding 20%. To reduce the levelized cost of electricity (LCOE) produced by the solar cells, a higher conversion efficiency must be realized; consequently, researchers have been developing several types of higher efficiency solar cells [1]. Passivated emitter and rear cell (PERC) [2] technologies are expected to become the mainstream standard for the photovoltaic (PV) market in the near future. Silicon hetero junction (SHJ) [3] shows the high voltage and the high conversion efficiency over 25% by adopting the amorphous Si and crystal Si hetero-junction. Interdigitated back contact (IBC) cells [4] have no metal lines at the front surface, which increases the photo-generated current density by solving the shadow loss problem. IBC-SHJ solar cells are the combination of SHJ and IBC [5], and they have realized the extremely high conversion efficiency of 26.33% [6]. On the other hand, although many studies have been conducted for the development of higher conversion efficiency, the cell structures of these solar cells are complicated, and consequently require more steps in the fabrication process. This increases the cost of solar cell fabrication. To solve this problem, passivated contact cells with simple structures but high conversion efficiency, such as tunnel-oxide passivated contact (TOPCon) [7] and carrier-selective contact (CSC) [8] cells, have been proposed.

In this paper, we will outline trends of recent high conversion efficiency crystalline Si solar cells, which are dramatically changing solar cell technologies and the PV market.

## HIGH CONVERSION EFFICIENCY CRYSTALLINE SI SOLAR CELLS

The conversion efficiency of present crystalline Si solar

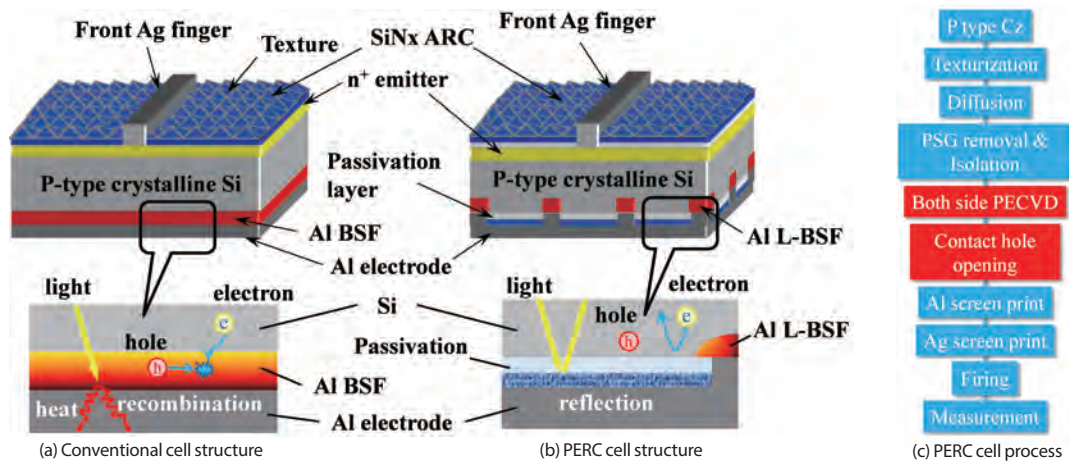


**Fig. 1:** (a) Schematic structure of a conventional solar cell, (b) PERC cell, and (c) the PERC cell fabrication process.

cells is limited due to minority carrier recombination loss. The defects with deep energy levels in the forbidden gap of the Si crystal/passivation layer interface act as efficient recombination centers. The minority carrier recombination rate at the metal/semiconductor interface is extremely high. They limit the short current density ( $J_{sc}$ ) and the open circuit voltage ( $V_{oc}$ ). The shadow loss also decreases the current density, because the contact metal lines at the front surface prevent light absorption. PERC, SHJ, IBC, and SHJ-IBC type cells solve these problems and consequently, higher conversion efficiencies have been realized. Hereafter, these high performance solar cells will be discussed.

**Passivated emitter and rear cell (PERC)**

PERCs can reduce the minority carrier recombination loss at the rear surface, and with this reduction, achieves a conversion efficiency over 20% [1]. In a conventional solar cell, boron (B) -doped p-type Si is used as a substrate and an Al-BSF (back surface field) layer is formed on the entire rear surface (Fig. 1 (a)). Although the Al-BSF layer decreases the minority carrier recombination rate, it still acts as a relatively active recombination region, which limits the conversion efficiency. Since the absorption coefficient of long wavelength light is small in Si crystals, some incident light reaches the back side of the

solar cell. The light reflectivity at the Al-BSF layer is low, and the light is efficiently absorbed there resulting in heat loss. On the other hand, PERCs have a passivation layer formed by an insulator, such as an oxide and/or nitride films, at the rear surface, which replaces Al-BSF (Fig. 1 (b)). This back-side passivated layer suppresses the recombination of minority carriers. The metal/passivated layer structure acts as a mirror which efficiently reflects long wavelength light, which increases the photo current. Laser ablation or chemical etching makes small-sized contact holes at the rear side. The electrodes of the front and back sides are formed by conventional screen printing and firing processes. The fabrication processes of standard PERCs are summarized in Fig. 1 (c). The blue parts represent the conventional cell fabrication process, and the red parts are steps that are added to the conventional process, for PERC. The current statuses of p-type mono- and multi- crystalline PERCs are listed at Tables I and II. High conversion efficiencies over 22% have been obtained by mono-crystalline PERCs. The selective emitter structure increased the conversion efficiency (22.61%) [9]. Multi-crystalline Si PERCs also show high conversion efficiencies of over 21% [12,13] and the highest efficiency of a multi-crystalline PERC module (19.86 %) has been realized by Trina Solar [13]. Since simply adding two or three steps makes it possible to fabricate a PERC

**Table I:** Current Status of high efficiency P-type mono-crystalline PERC.

Organization	Efficiency	Notes
Trina Solar	22.61%	Selective Emitter (2016) [9]
SolarWorld	22.04%	(2015) [10]
Hanwha Q Cells	22.00%	Average cell efficiency: 21.4% (2016) [11]

**Table II:** Current Status of high efficiency P-type multi-crystalline PERC.

Organization	Efficiency	Notes
Jinko Solar	21.63%	Average cell efficiency: 21.1% (2016) [12]
Trina Solar	21.25%	Module efficiency: 19.86% (2016) [13]
Hanwha Q Cells	20.90%	Module efficiency: 19.5% (2016) [14]

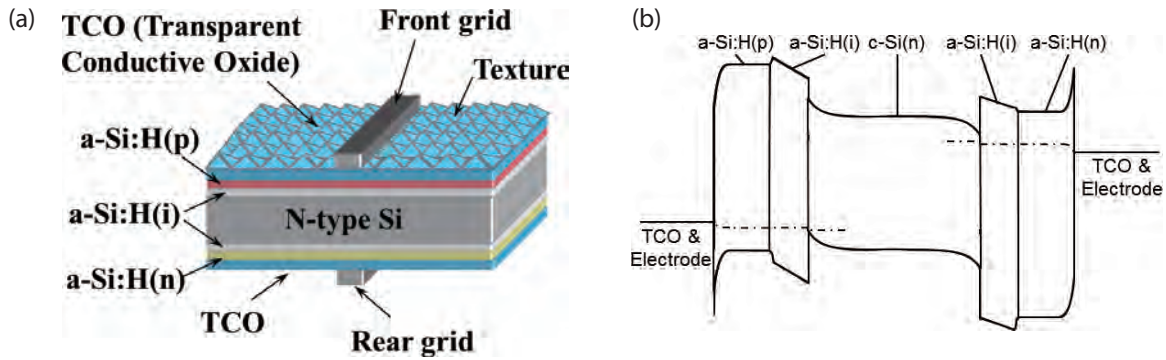


Fig. 2: (a) Schematic image of SHJ cell structure and (b) the band diagram.

structure, cell manufacturers can renew their production lines by making full use of existing conventional cell production facilities. In other words, it is also a great benefit for cell manufacturers that the capital investment can be minimized. Due to these merits, PERC cell technologies have rapidly improved and they are mass-produced all over the world at present.

**Silicon hetero junction (SHJ) cell**

A schematic image of SHJ cell structure is shown in Fig. 2(a). A SHJ solar cell realizes a high conversion efficiency of over 25% because of the hetero junction, which consists of a p-type hydrogenated amorphous Si (a-Si:H(p))/insulator a-Si:H (a-Si:H(i))/n-type crystal Si, and n-type hydrogenated amorphous Si (a-Si:H(n))/insulator a-Si:H (a-Si:H(i))/n-type crystal Si. The original idea has been realized as the HIT solar cell by Sanyo Corporation [3]. N-type crystalline Si is used as a substrate. The a-Si:H(n)/a-Si:H(i) for the electron contact and a-Si:H(p)/a-Si:H(i) for the hole contact are deposited by plasma-enhanced chemical vapor deposition (CVD) using SiH<sub>4</sub> as a source gas. Transparent conductive material, such as ITO (indium tin oxide), is deposited on them, and then the metal electrodes are formed. The band-structure of this solar cell is shown in Fig. 2(b). Photo-generated carriers in the Si crystal are extracted to the electrode via a-Si:H layers and ITO. The carrier transport mechanism across the crystal/amorphous junction is considered to be thermionic emission and trap-assisted tunneling [15]. This

hetero structure achieves high carrier selectivity. There is no direct contact between the metal and semiconductor, and the a-Si:H(i) layers act as high quality surface passivation at the interfaces, which almost realize the intrinsic recombination limit of the high quality crystalline Si. The carrier selectivity and the high quality passivation realize the excellent high open circuit voltage ( $V_{oc}$ ) above 700mV. The resistivity of the doped amorphous layer, the defects densities and these energy levels in the a-Si:H(i) film and at the interface between it and Si crystal determine the solar cell properties. However, from a theoretical viewpoint, the conventional carrier transportation model fails to explain the  $V_{oc}$  dependence on the thickness of an i-layer, meaning that there are still unknown issues in the device physics [16]. The current status of efficiency is listed at Table III. Because the SHJ cell has several advantages - for example, high  $V_{oc}$  and high conversion efficiency, a cell manufacturing process at a relatively low temperature (200°C or lower) and good temperature characteristics - various companies and research institutions are actively working on the technology, development and mass production of these cells.

**Interdigitated back contact (IBC) cell**

IBC cell structure is shown in Fig. 3. An IBC cell, which has no metal grid at the front surface, generates high photo-induced current density. This realizes high efficiency of over 20%. The shadow loss due to the front grids in conventional and PERC cell structures decrease

Table III: Current status of high efficiency SHJ cells.

Organization	Efficiency	Notes
KANEKA	25.1%	Cu plating electrode [17], Module efficiency: 22.2% (2015) [18]
Panasonic	24.7%	Screen printing electrode, Module efficiency: 22.5% (2015) [19]
SIMIT, Trina Solar	22.95%	Screen printing electrode, Cell area: 154cm <sup>2</sup> (2015) [20]

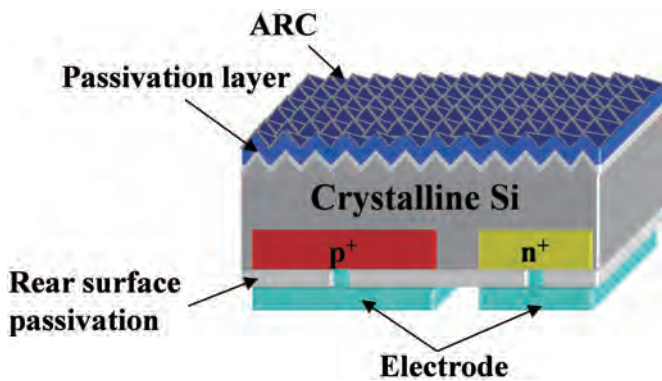


Fig. 3: Schematic image of IBC cell structure.

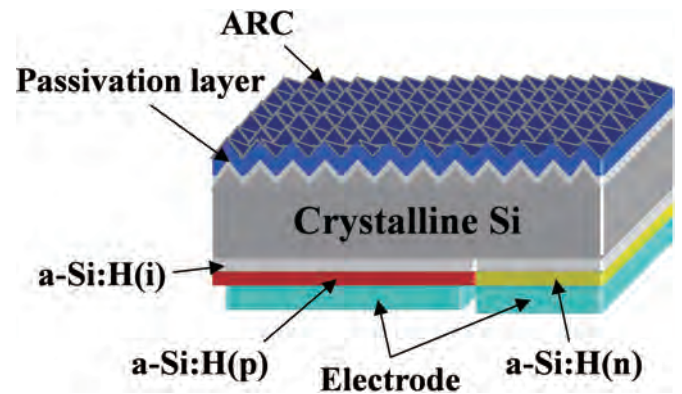


Fig. 4: Schematic image of IBC-SHJ cell structure.

the amount of current generated by the solar cell. As a substrate, n-type Si is widely used. An IBC solar cell has many localized junctions at the rear, instead of a single large p-n junction. This suppresses the light shielding and allows 100% sunlight absorption on the front-side. The contact areas are as small as possible to reduce recombination at the metal/semiconductor interface. Then, the higher  $J_{sc}$  can be obtained. The photo-generated minority carrier is transported horizontally. This requires high quality Si crystals, which allow the long diffusion length of the carriers. To prevent minority carrier recombination at the front surface, good quality passivation is required. Despite the disadvantages due to the fact that the cell fabrication process is complicated because of its characteristic structure, the advantages of high efficiency are apparent from the current status of the development of high efficiency IBC cells. The current status of high efficiency IBC cells is listed at Table IV.

### IBC-SHJ cell

If high  $V_{oc}$ , which is a feature of the SHJ cell, and high  $J_{sc}$ , which is a characteristic of the IBC cell, can be satisfied at the same time, a crystalline silicon solar cell with higher efficiency can be realized. An IBC-SHJ cell was developed from such an idea. As shown in Fig. 4, a-Si:H is used to make an IBC structure without the electrodes on the light receiving surface in the IBC-SHJ cell structure. Table V shows the development status of the high efficiency IBC-SHJ cells. Since 1999, the world record

for crystalline silicon solar cell conversion efficiency was 25.0% [26, 27]. However, Panasonic achieved cell efficiency of 25.6% in an IBC-SHJ cell in 2014 and updated the world record for efficiency for the first time in 15 years. KANEKA has achieved a further high of 26.33% in 2016 [6], and this renewed world record proves the high potential of the IBC-SHJ cell.

### FUTURE GENERATION SOLAR CELLS

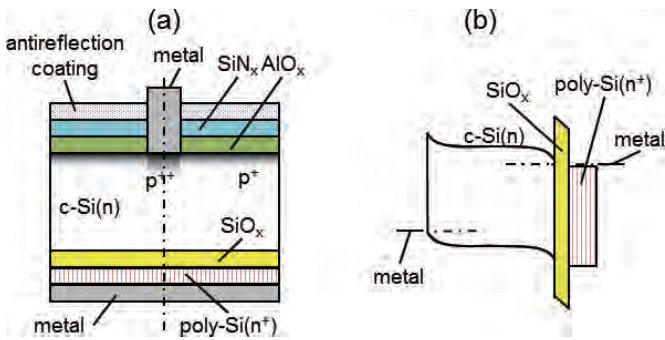
Although IBC-SHJ cells have realized high conversion efficiency, there still remain some problems from the viewpoint of mass production. These high efficiency solar cells require many steps in the process of fabrication, and some of them have narrow process windows. For example, to make a heterojunction, the plasma-enhanced CVD (P-CVD) process is used. Extremely high quality surface cleaning is required before the a-Si:H deposition, to realize very high performance of passivation. The P-CVD process temperature should be limited to under 250 °C in order to prevent a-Si:H layer crystallization. However, this low temperature limits the conditions of other processes, which causes the insufficient properties of others. The deposited film thickness of the a-Si:H(i) layer must be precisely controlled, and be less than 10 nm. This optimal thickness range is determined based on the balance between the carrier transport and the passivation quality associated with this a-Si:H(i) layer. This increases the fabrication cost and also causes difficulties in obtaining the

Table IV: Current status of high efficiency IBC cells.

Organization	Efficiency	Notes
SunPower	25.2%	Passivated Contact, Plating electrode (2015) [21]
Trina Solar, ANU	24.4%	Cell area: 4.00 cm <sup>2</sup> (2014) [22]
Trina Solar	23.5%	Screen printing electrode, Cell area: 238.6 cm <sup>2</sup> (2016) [23]

Table V: Current status of high efficiency IBC-SHJ cells.

Organization	Efficiency	Notes
KANEKA	26.33%	Module efficiency: 24.37% (2016) [6]
Panasonic	25.6%	Cell area: 143.7 cm <sup>2</sup> (2014) [24]
SHARP	25.1%	Cell area: 3.713 cm <sup>2</sup> (2014) [25]



**Fig. 5:** (a) Schematic image of a TOPCon a cell with an n-type substrate and (b) the band structure.

expected properties of SHJ and IBC-SHJ, and thus only a few research groups have been able to realize high-performance SHJ cells with efficiency nearing 25%. To solve the above mentioned problems, new solar cells based on the passivated contact concept, such as tunnel-oxide passivated contact (TOPCon) and the carrier-selective contact (CSC) cells, have been proposed.

**Tunnel oxide passivated contact (TOPCon) cell**

The tunnel oxide passivated contact (TOPCon) cell was proposed by Fraunhofer ISE [7]. A schematic image of a TOPCon cell with an n-type substrate is shown in Fig. 5. At the front surface, a B-doped emitter is fabricated by a conventional thermal diffusion process. At the rear surface, a Si oxide layer with less than 5 nm thickness is inserted between the Si substrate and doped poly-crystalline Si layer. No direct contact between the metal and semiconductor Si prevents severe minority carrier recombination at the contact region, resulting in the low reverse saturation current ( $J_0$ ) in the diode characteristic. The contact at the back surface acts as the well electron-selective contact. Photo-generated electrons in the Si substrate are considered to be extracted via a tunneling mechanism through the tunnel oxide to the doped Si [28]. Meanwhile, hole transportation is prevented due to the large difference between the Si crystal and the doped Si work functions. They increase the  $I_{sc}$  and  $V_{oc}$ . TOPCon cells show high potential as highly efficient cells, realizing over 25 % [29]. All back contact type TOPCon cells will increase conversion efficiency, although the fabrication technique is rather difficult and the production costs become high. There has been an attempt to use an ion implantation technique in order to make a back contact pattern design, which achieved a high implied  $V_{oc}$  of 710 mV [30].

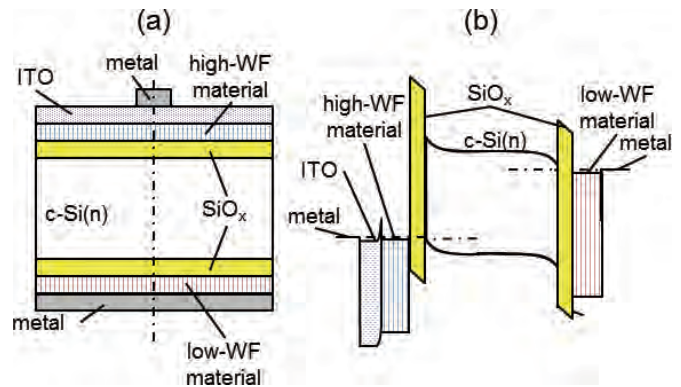


**Fig. 6:** (a) Typical cell structure of a CSC cell and (b) the band structure. In a front-side, a high work function (WF) material is used as a hole contact, while a low WF material as an electron contact.

**Carrier-selective contact (CSC) cells**

Carrier-selective contact (CSCs) cells are expected to realize higher conversion efficiency crystalline Si solar cells with lower fabrication costs, because of their simple cell structure. The typical cell structure and a band diagram for a CSC cell are shown in Fig. 6. The thin  $SiO_2$  layers are formed at the both surfaces of a Si substrate. As discussed in TOPCon, this  $SiO_2$  and Si interface shows good passivation quality and prevents minority carrier recombination. The thickness of  $SiO_2$  is less than 5 nm, which allows carrier transportation through this layer because of the tunneling mechanism. On these  $SiO_2$  layers, the contact materials are deposited. The work function difference between the Si and electrode material determines the band bending at the Si surface. A large work function material, with an energy level below that of the energy of the valence band maximum, is required for a hole-selective contact. A small work function material, with an energy level around the energy of the conduction band minimum, is used for an electron-selective contact. The relation between the cell properties and work function of the contact material is shown in Fig. 7. This was obtained by a device simulation, assuming that an n-type Si substrate thickness was smaller than the carrier diffusion length, and that the direct tunneling through 1.6nm  $SiO_2$  determines the carrier transportation and the recombination velocity at Si/ $SiO_2$  interface was zero. For the hole contact (black plots), the work function of the rear side contact material (rear WF) is the parameter. For the electron contact (white plots), the work function of the front side contact material (front WF) is the parameter. The combination of high and low work function contact material is required for high  $V_{oc}$ . The result indicates that for the hole contact, the work function of the electrode material will be over

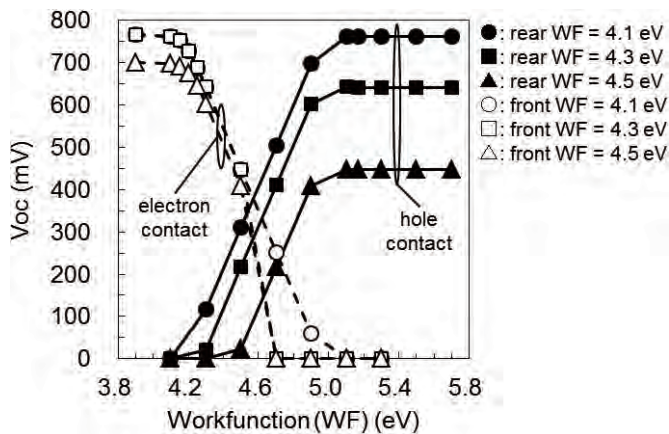


**Fig. 7:** Relationship between the cell performance ( $V_{oc}$ ) and work function (WF) of the contact material in the CSC cell.

5.3eV, and that for the electron contact, an amount below 4.1eV is required. For realizing CSC solar cells, the following high work function transition-metal oxides, such as, molybdenum oxide (MoOx) [31-34], vanadium oxide (VOx) [34, 35], tungsten oxide (WOx) [34, 36], and other compounds, CuI [37,38] and SiC [39], have been widely studied as the hole contact materials. As the low work function materials, TiOx [40], SnOx [41], LiFx [32] are some of the candidates for the electron contact.

## SUMMARY

The conversion efficiencies of crystalline silicon solar cells are increasing and the module costs have dramatically lowered. PERCs with over 20% efficiency became the next generation crystalline Si solar cell for mass-production. Hetero-junctions increased the open circuit voltage and back contacts realized the high density of photo-induced currents. By combining these advanced features, IBC-SHJ achieved high conversion efficiency of 26.33%. As future solar cells, passivated contact cells were proposed. It is believed that they will decrease fabrication costs, while high conversion efficiency will be obtained. On the other hand, the quality of crystal Si, metal contamination during cell fabrication, and damages induced by the processes, are critical issues to overcome in order to realize the mass-production of these high conversion efficiency solar cells. To realize the higher conversion efficiency and lower cost crystalline Si solar cells of the future, fundamental and deep knowledge about these issues are important, and collaboration between universities, national institutes and companies is strongly required.

**Acknowledgements:** The authors are grateful for the support provided by the Ministry of Education, Culture, Sports, Science and Technology and by the New Energy and Industrial Technology Development Organization (NEDO) under the Ministry of Economy, Trade and Industry (METI).

## References

- [1] International Technology Roadmap for Photovoltaic Results 2015 including maturity report. <http://www.itrpv.net/Reports/Downloads/2016/> (accessed 2017-01-26).
- [2] A. W. Blakers, A. Wang, A. M. Milne, J. Zhao, and M. A. Green, *Appl. Phys. Lett.*, 55, 1363 (1989).
- [3] M. Tanaka, S. Okamoto, S. Tsuge and S. Kiyama, *Proc. 3rd World Conf. Photovoltaic Energy Convers.*, 955 (2003).
- [4] M. D. Lammert, and R. J. Schwartz, *IEEE Transactions on Electron Devices*, 24, 337 (1977).
- [5] M. Lu, S. Bowden, U. Das, and R. Birkmire, *Applied Physics Letters*, 91(063507), 1 (2007).
- [6] Kaneka Corporation News Release. World's Highest Conversion Efficiency of 26.33% Achieved in a Crystalline Silicon Solar Cell [http://www.kaneka.co.jp/kaneka-e/images/topics/1473811995/1473811995\\_101.pdf](http://www.kaneka.co.jp/kaneka-e/images/topics/1473811995/1473811995_101.pdf) (accessed 2017-01-26).
- [7] F. Feldmann, M. Bivour, C. Reichel, M. Hermle, S. W. Glunz, *Sol. Energy Mat. Sol. Cells*, 120, 270 (2014).
- [8] J. Bullock, Y. Wan, M. Hettick, J. Geissbühler, A. J. Ong, D. Kiriya, D. Yan, T. Allen, J. Peng, X. Zhang, C. M. Sutter-Fella, S. D. Wolf, C. Ballif, A. Cuevas, and A. Javey, *Proc. 43rd IEEE Photovoltaic Specialists Conference (PVSC)*, 0210 (2016).
- [9] Trina Solar Press Release. Trina Solar Announces New Efficiency Record of 22.61% for Mono-Crystalline Silicon PERC Cell. <http://ir.trinasolar.com/phoenix.zhtml?c=206405&p=irol-newsArticle&iD=2230468> (accessed 2017-01-26).
- [10] rheatsao (2016). SolarWorld's P-type Mono PERC Cell Hits 22.04% Efficiency. *Energy Trend*. [http://pv.energytrend.com/news/SolarWorld\\_P\\_type\\_Mono\\_PERC\\_Cell\\_Hits\\_22\\_04\\_percent\\_Efficiency.html](http://pv.energytrend.com/news/SolarWorld_P_type_Mono_PERC_Cell_Hits_22_04_percent_Efficiency.html) (accessed 2009-12-03).
- [11] M. Schaper, J. Cieslak, K. Duncker, C. Fahrland, S. Geissler, S. Hörnlein, C. Klenke, R. Lantzsch, A. Mohr, L. Niebergall, A. Schönmann, M. Schütze, J.W. Müller, and D.J.W. Jeong: presented at 32nd European Photovoltaic Solar Energy Conference, 2016.
- [12] H. Jin, P. Zheng, H. Sun, J. Xu, F. Zhang, Y. Guo: presented at 26th International Photovoltaic Science & Engineering Conference, 2016.
- [13] P. Verlinden: presented at 26th International Photovoltaic Science & Engineering Conference, 2016.
- [14] M. Scherff, P. Kowalzik, C. Gerber, K. Duncker, M. Junghänel, C. Fahrland, S. Kunath, S. Hörnlein, M. Schütze, L. Niebergall, B. Klöter, and J.W. Müller: presented at 32nd European Photovoltaic Solar Energy Conference, 2016.
- [15] A. Kanevce and W. K. Metzger, *J. Appl. Phys.*, 105, 094507 (2009).
- [16] Y. Hayashi, D. Li, A. Ogura, and Y. Ohshita, *IEEE J. Photovoltaics*, 3 1149 (2013).
- [17] K. Yamamoto, D. Adachi, H. Uzu, T. Uto, T. Irie, M. Hino, M. Kanematsu, H. Kawasaki, K. Konishi, R. Mishima, K. Nakano, T. Terashita, K. Yoshikawa, M. Ichikawa, T. Kuchiyama, T. Suezaki, T. Meguro, N. Nakanishi, M. Yoshimi, D. Schroos, N. Valckx, N. Menou, J. L. Hernández: *Proc. 31st European Photovoltaic Solar Energy Conference*, 3CP.1.1. (2015).
- [18] T. Uto, D. Adachi, M. Kanematsu, K. Nakano, T. Irie, T. Asatani, T. Terashita, T. Meguro, N. Nakanishi, M. Yoshimi, J. L. Hernández, D. Schroos, N. Valckx,

- N. Menou, K. Yamamoto: Abstr. 25th International Photovoltaic Science & Engineering Conference, Csi-O-15, (2015).
- [19] M. Taguchi, S. Okamoto: Abstr. 25th International Photovoltaic Science & Engineering Conference, Plenary Lecture 2, (2015).
- [20] J. Yu, J. Bian, Y. Liu, F. Meng, Z. Liu: Abstr. 25th International Photovoltaic Science & Engineering Conference, Csi-O-17, (2015).
- [21] M. A. Green, K. Emery, Y. Hishikawa, W. Warta, and E. D. Dunlop: Prog. Photovolt: Res. Appl.; 24 905 (2016).
- [22] Trina Solar Press Release. Trina Solar and ANU Jointly Develop High Efficiency Solar Cell. [http://ir.trinasolar.com/phoenix.zhtml?c=206405&p=irol-newsArticle\\_print&ID=1904732&highlight=\(accessed 2017-01-26\)](http://ir.trinasolar.com/phoenix.zhtml?c=206405&p=irol-newsArticle_print&ID=1904732&highlight=(accessed 2017-01-26)).
- [23] Z. Li, Y. Yang, X. Zhang, W. Liu, Y. Chen, G. Xu, X. Shu, Y. Chen: Proc. 32nd European Photovoltaic Solar Energy Conference, 2DO.16.3, (2016).
- [24] Panasonic Press Release. Panasonic HIT® Solar Cell Achieves World's Highest Energy Conversion Efficiency of 25.6% at Research Level <http://news.panasonic.com/global/press/data/2014/04/en140410-4/en140410-4.html> (accessed 2017-01-26).
- [25] J. Nakamura, N. Asano, T. Hieda, C. Okamoto, H. Katayama, and K. Nakamura: IEEE Journal of Photovoltaics, 4, 1491(2014).
- [26] J. Zhao, A. Wang, M. A. Green, Progress in Photovoltaics 7, 471 (1999).
- [27] M. A. Green, Progress in Photovoltaics, 17, 183 (2009).
- [28] H. Steinkemper, F. Feldmann, M. Bivour, and M. Hermle, IEEE J. Photovoltaics, 5, 1348 (2015).
- [29] S. W. Glunz, F. Feldmann, A. Richter, M. Bivour, C. Reichel, H. Steinkemper, J. Benick, M. Hermle, Proc. 31st European Photovoltaic Solar Energy Conference and Exhibition, 259 (2015).
- [30] C. Reichel, F. Feldmann, R. Müller, A. Moldovan, M. Hermle, S. W. Glunz, Proc. 29th European PV Solar Energy Conference and Exhibition, 487-491(2014).
- [31] C. Battaglia, S. Martin de Nicolás, S. D. Wolf, X. Yin, M. Zheng, C. Ballif, and A. Javey, Appl. Phys. Lett., 104, 113902 (2014).
- [32] J. Bullock, M. Hettick, J. Geissbühler, A. J. Ong, T. Allen, C. M. Sutter-Fella, T. Chen, H. Ota, E. W. Schaler, S. D. Wolf, C. Ballif, A. Cuevas, and A. Javey, Nature Energy, 1, 15031 (2016).
- [33] M. Bivour, B. Macco, J. Temmler, W. M. M. Erwin Kessels, and M. Hermle, Energy Procedia, 92, 443 (2016).
- [34] L. G. Gerling, S. Mahato, A. M.-Vilches, G. Masmija, P. Ortega, C. Voz, R. Alcubilla, and J. Puigdollers, Sol. Energy Mat. Sol. Cells, 145, 109 (2016).
- [35] L. G. Gerling, G. Masmija, C. Voz, P. Ortega, J. Puigdollers, and R. Alcubilla, Energy Procedia, 92, 633 (2016).
- [36] M. Mews, L. Korte, and Bernd Rech, Sol. Ener. Mat. Sol. Cells, 158, 77 (2016).
- [37] J. A. Christians, R. C. M. Fung, and P. V. Kamat, J. Am. Chem. Soc., 136, 758 (2014).
- [38] S. A. Mohamed, J. Gasiorowski, K. Hingerl, D. R. T. Zahn, M. C. Scharber, S. S. A. Obayya, M. K. El-Mansy, N. S. Sariciftci, D. A. M. Egbe, and P. Stadler, Sol. Energy Mat. Sol. Cells, 143, 369 (2015).
- [39] G. Nogay, J. Stuckelberger, P. Wyss, Q. Jeangros, C. Allebé, X. Niquille, F. Debrot, M. Despeisse, F.-J. Haug, P. Löper, and C. Ballif, Appl. Mater. Interfaces, 8, 35660 (2016).
- [40] K. A. Nagamatsu, S. Avasthi, G. Sahasrabudhe, G. Man, J. Jhaveri, A. H. Berg, J. Schwartz, A. Kahn, S. Wagner, and J. C. Sturm, Appl. Phys. Lett., 106, 123906 (2015).
- [41] J. Song, E. Zheng, X.-F. Wang, W. Tian, Y. Sanehira, and T. Miyasaka, J. Mater. Chem. A, 3, 10837 (2015).
- [42] H.-D. Um, N. Kim, K. Lee, I. Hwang, J.-H. Seo, and K. Seo, Nano Lett., 16, 981 (2016).



Professor **Yoshio Ohshita** is a Professor at Toyota Technological Institute. He received the Doctor of Engineering degree in Electronics from Nagoya University in 1991. He worked for NEC Corporation in 1985 – 1999, as a researcher of ULSI device technologies and materials. In 2000, he joined the Semiconductor Laboratory at Toyota Technological Institute as an associate professor. The solar cell devices and materials are his main research target. To realize four junction tandem ones, the chemical beam epitaxial growth technology was developed and good quality of GaAsN material was obtained. He also focuses on the development of the crystalline silicon solar cells. He is researching some new technologies and materials to increase the conversion efficiency and to decrease the cost under the New Energy Development Organization (NEDO) project.



**Takefumi Kamioka** received his PhD in engineering in 2009 from Waseda University. He worked on the carrier transport mechanism in nano-scale transistor by means of a molecular dynamics based simulation as a postdoc. He joined Toyota Technological Institute since 2014. He has been working on the development of crystalline Si heterojunction solar cells. Current research interests are the modeling and simulation, characterization of the related device physics.



**Kyotaro Nakamura** is a Project Professor of Meiji University in Japan. After 9 years business career at Sharp Corporation, he went to Graduate School of Osaka University, and received Ph.D. in 2002. Then, he reentered Sharp Corporation and has engaged to develop high efficiency and low cost crystalline Si solar cells for 11 years. After retirement at the end of 2012, he worked as a researcher in Toyota Technology Institute for 4 months, and then, transferred to Meiji University. His main interest is development of high efficiency low cost and high reliability crystalline Si PV.